

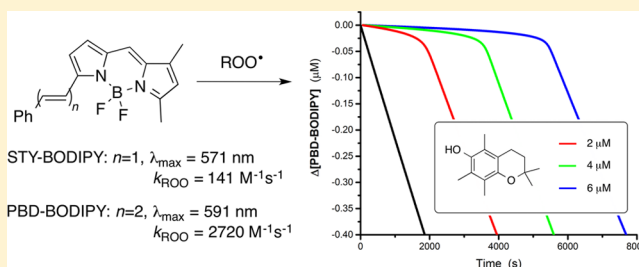
A Continuous Visible Light Spectrophotometric Approach To Accurately Determine the Reactivity of Radical-Trapping Antioxidants

Evan A. Haidasz, Antonius T. M. Van Kessel, and Derek A. Pratt*

Department of Chemistry and Biomolecular Sciences, University of Ottawa, Ottawa, Ontario, K1N 6N5, Canada

S Supporting Information

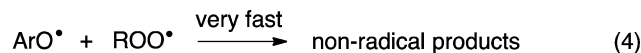
ABSTRACT: Inhibited autoxidations—monitored either by O₂ consumption or hydroperoxide formation—are the most reliable way to obtain kinetic and stoichiometric information on the activity of radical-trapping antioxidants (RTAs). While many comparatively simple “antioxidant assays” (e.g., the DPPH assay) have supplanted these in popularity, they are generally *very poor* substitutes since they often do not employ peroxy radicals as the oxidant and do not account for both the kinetics and stoichiometry of the radical-trapping reaction(s). In an effort to make inhibited autoxidations as simple as the most popular “antioxidant assays”, we have developed a spectrophotometric approach for monitoring reaction progress in inhibited autoxidations. The approach employs easily prepared 1-phenylbutadiene-conjugated or styrene-conjugated BODIPY chromophores (PBD-BODIPY or STY-BODIPY, respectively) as signal carriers that co-oxidize along with a hydrocarbon substrate. We show that inhibition rate constants (*k_{inh}*) are accurately determined for a range of phenolic and diarylamine RTAs using this approach and that mechanistic experiments, such as kinetic isotope effects and kinetic solvent effects, are equally easily carried out. Moreover, synergistic interactions between RTAs, as well as the unconventional activity of diarylamine RTAs, are captured using this methodology. Lastly, we show that the approach can be employed for monitoring reactions in aqueous solution.



INTRODUCTION

Autoxidation, the radical-mediated chain reaction that converts hydrocarbons to hydroperoxides (eqs 1 and 2, Scheme 1), can

Scheme 1. Chain-Propagating Steps of Hydrocarbon Autoxidation (eqs 1 and 2) and Its Inhibition by a Phenolic Radical-Trapping Antioxidant (eqs 3 and 4)



be inhibited by the addition of radical-trapping antioxidants (RTAs). The relevant inhibition reactions for phenolic RTAs are shown in eqs 3 and 4 (Scheme 1). The inherent reactivity of an RTA is characterized by the rate constant for its reaction with peroxy radicals (also known as the inhibition rate constant, *k_{inh}*) since this is the reaction that competes with the rate-determining propagation step of the chain reaction (eq 1). An additional, but equally important, consideration is the stoichiometry of the RTA-peroxy reaction (*n*), which is generally 2 for phenols due to the reactions in eqs 3 and 4.^{1,2}

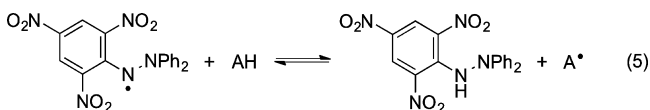
Given the importance of RTAs in the preservation of petroleum-derived materials and consumer products, as well as

their putative role in maintaining human health and promoting longevity, many methods have been developed to study RTAs. The best approaches comprise kinetic studies of inhibited autoxidations, where reaction progress is followed either by consumption of one of the starting materials (O₂) or the formation of products (hydroperoxides).^{3–5} The former approach is preferred as it can be carried out continuously, but it involves specialized equipment to accurately assess the pressure differential between inhibited and uninhibited autoxidations carried out in parallel. The latter approach is a discontinuous assay where hydroperoxides are determined in aliquots removed from the reaction mixture. This is usually done by laborious iodometric titrations or time-consuming chromatographic analyses. Recently developed fluorogenic probes are attractive alternatives, but the fact remains that these are discontinuous assays.⁶

Over the years, the desire for more accessible and/or rapid alternatives to inhibited autoxidations has prompted the development of a myriad of assays of “antioxidant activity”. Some of the most common include TROLOX equivalent antioxidant capacity (TEAC),⁷ ferric reducing antioxidant power (FRAP),⁸ and DPPH• quenching (eq 5).^{9–11} These approaches are generally based on spectrophotometric determination of the position of the equilibrium between a test antioxidant (a reducing agent) and an oxidizing agent that

Received: September 16, 2015

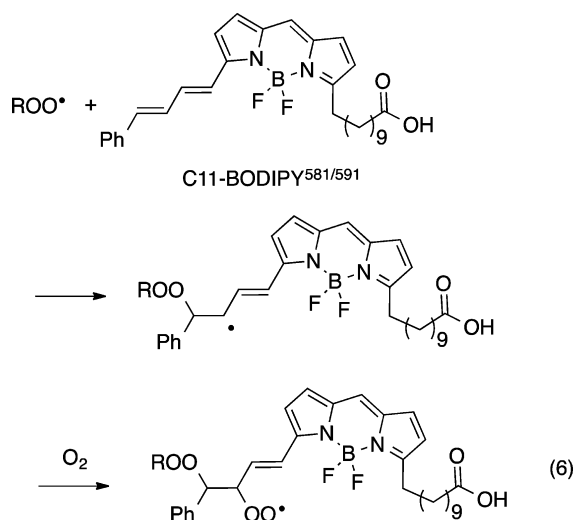
Published: November 3, 2015



possesses a good absorbance and/or fluorescence.^{3–5} It must be emphasized that *peroxyl radicals are often not employed as the oxidizing agent* in these experiments and that they are generally carried out in highly polar (alcoholic) solvents that are necessary to solubilize the reagents. *Such solvents are poor models for either the confines of the lipid bilayer or petroleum-derived materials wherein RTA activity is most important.* In fact, these reactions can be subject to kinetic solvent effects owing to either H-bonding of the RTA or the contributions of electron-transfer reactions from the conjugate base of the RTA.¹² The ideal approach to determine the reactivity of RTAs would incorporate the desirable features of the above methods; it would be rapid, operationally simple, utilize standard laboratory equipment, and most importantly be capable of providing accurate kinetic and stoichiometric information for reactions of RTAs with peroxyl radicals.

C11-BODIPY^{581/591} is a popular compound for monitoring lipid oxidation in cell culture.^{13,14} Its fluorescence is shifted significantly (from 595 to 520 nm) upon reaction with peroxyl radicals—presumably as a result of reduced conjugation due to peroxyl radical addition to the 4-phenyl-1,3-butadienyl (PBD) unit followed by O₂ addition to the resultant carbon-centered radical as shown in Scheme 2 (although this has not been studied in detail).

Scheme 2. Propagation Steps in the Autoxidation of C11-BODIPY^{581/591}.

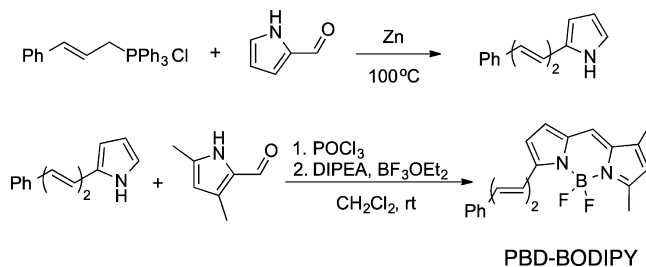


Niki¹⁵ demonstrated that C11-BODIPY^{581/591} is oxidized in azo-initiated co-oxidations with methyl linoleate and that an added antioxidant (2,6-di-*tert*-butyl-4-methylphenol, BHT) can slow this process. Accordingly, we wondered if an assay based upon the competitive oxidation of C11-BODIPY^{581/591} (or a suitable inexpensive analogue thereof) and an appropriate organic substrate (to ensure that the process is a radical chain reaction) could be developed to enable the accurate determination of the inhibition rate constants (k_{inh}) and stoichiometry (n) of reactions of RTAs with peroxyl radicals. Our successful efforts are described below.

RESULTS AND DISCUSSION

Since the undecanoic acid substitution in C11-BODIPY^{581/591} simply provides fatty acid-like physical properties for

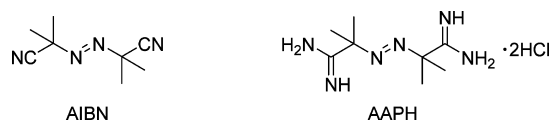
Scheme 3. Synthesis of PBD-BODIPY



phospholipid bilayer solubility, the solution-based experiments described here were performed with the simpler BODIPY-substituted 1-phenylbutadiene (hereafter PBD-BODIPY). This compound is much more easily prepared (Scheme 3)^{16,17} and manipulated than the commercially available (but exceedingly expensive) C11-BODIPY^{581/591}. The spectroscopic properties of PBD-BODIPY have been described by others^{16,17} and are highly similar to that of C11-BODIPY^{581/591},¹⁸ in particular, the absorption spectrum, which features a maximum at 591 nm and emission spectrum with corresponding maximum at 608 nm.⁴

Under conditions similar to those commonly used in O₂ consumption experiments, the AIBN-initiated (see Chart 1)

Chart 1. Radical Initiators Used in This Work



co-oxidation of styrene (4.3 M in chlorobenzene) and PBD-BODIPY (10 μM) at 37 °C, produced a linear increase in fluorescence at 515 nm with time ($\lambda_{\text{ex}} = 485$ nm, data not shown). However, since PBD-BODIPY is expected to oxidize in a similar manner to styrene—via addition of a peroxyl radical to the phenylbutadienyl unit followed by O₂ addition to the resultant alkyl radical to afford a new peroxyl radical (as shown for C11-BODIPY^{581/591} in eq 6)¹⁹—the fluorescent product is incorporated into a styrene-oxygen copolymer in solution, precluding standardization of the signal.²⁰ Therefore, we elected to monitor the kinetics of PBD-BODIPY oxidation and its inhibition by added RTAs using absorbance. Representative examples are shown in Figure 1.

The reaction profiles in Figure 1 are strikingly reminiscent of those obtained from inhibited autoxidations monitored by O₂ consumption.^{3–5} Inhibition by the representative phenolic RTAs 1–4 followed the expected trend, where pyrimidinol 4 was most reactive to peroxyl radicals, suppressing PBD-BODIPY oxidation to the greatest extent, followed closely by 2,2,5,7,8-pentamethylchroman-7-ol (PMC, 3) and then 3,5-di-*tert*-butyl-4-hydroxyanisole (2) and, last, 3,5-di-*tert*-butyl-4-hydroxytoluene (BHT, 1).

Although a simple comparison of the initial rates of PBD-BODIPY consumption in the presence of the different RTAs provides a good qualitative assessment of their relative RTA activity, we sought to develop a method to obtain quantitative data, i.e., the inhibition rate constant (k_{inh}) for reaction of an RTA with peroxyl radicals. In order to do so, the rate constant for the competing reaction of PBD-BODIPY with peroxyl radicals ($k_{\text{PBD-BODIPY}}$) must be known. This was easily determined by measuring its rate of consumption in co-oxidations with variable concentrations of PBD-BODIPY (assuming a steady-state concentration of peroxyl radicals) via eq 7.^{3–5}

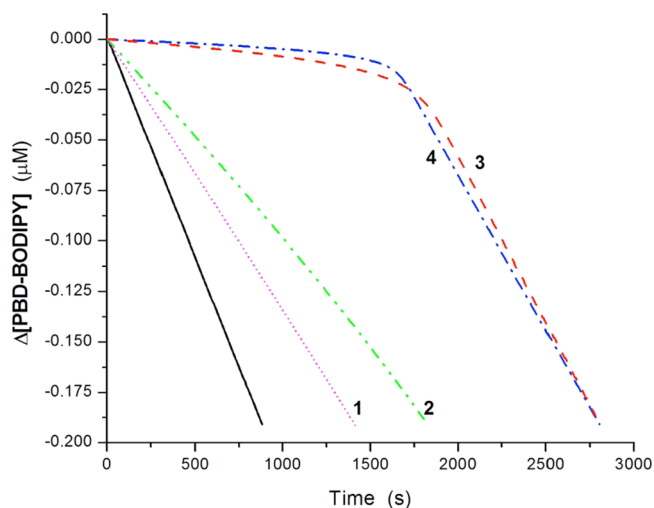
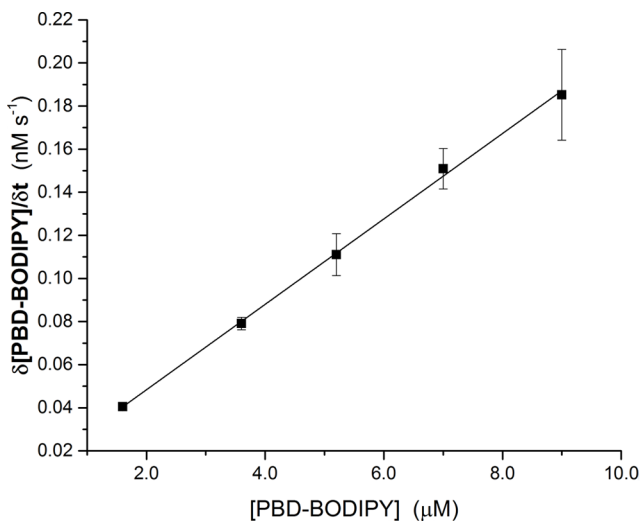


Figure 1. Co-oxidation of styrene (4.3 M) and PBD-BODIPY (10 μM) initiated by AIBN (6 mM) in PhCl at 37 $^{\circ}\text{C}$ (solid line) and inhibited by 2 μM BHT (1), BHA (2), PMC (3), and 2-(*N,N*-dimethylamino)-4,6-dimethyl-5-pyrimidinol (4). Reaction progress was monitored by absorbance at 591 nm ($\epsilon = 139,000 \text{ M}^{-1} \text{ cm}^{-1}$).

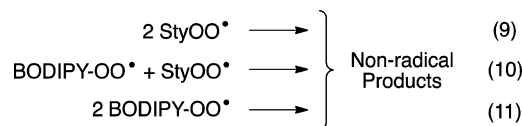
$$\frac{-\delta[\text{PBD-BODIPY}]}{\delta t} = \frac{k_{\text{PBD-BODIPY}}}{\sqrt{2k_t}} \sqrt{R_i} [\text{PBD-BODIPY}] \quad (7)$$

Thus, plotting the rate of PBD-BODIPY consumption versus its concentration (as in Figure 2) yields a line where the slope is given by a combination of $k_{\text{PBD-BODIPY}}$, $\sqrt{R_i}$, and $\sqrt{2k_t}$ (eq 7). The rate of initiation, R_i , can be estimated from literature data to be $2.0 \times 10^{-9} \text{ M s}^{-1}$ at 37 $^{\circ}\text{C}$. Alternatively, it can be determined readily under the exact experimental conditions simply from the length of the inhibition period, t_{inh} , of an inhibited autoxidation with a known amount of inhibitor AH, provided its stoichiometric number (n) is known, as in eq 8.

$$R_i = \frac{n[\text{AH}]}{t_{\text{inh}}} \quad (8)$$



Doing so with 3 (e.g., using the data in Figure 1), which is well-known to have $n = 2$, we obtain $R_i = 2.2 \times 10^{-9} \text{ M s}^{-1}$ corresponding to $ek_d = 1.9 \times 10^{-7} \text{ s}^{-1}$. Although there are three possible peroxy–peroxy radical termination reactions that may occur (eqs 9–11), we can assume that eq 9 dominates since styrylperoxy radicals react very rapidly with each other ($k_t = 2.1 \times 10^7 \text{ M}^{-1} \text{ s}^{-1}$)^{23,24} and styrene is present in a great excess compared to PBD-BODIPY.



Using these values of R_i and k_t , the rate constant for the reaction of PBD-BODIPY and peroxy radicals can be calculated as $k_{\text{PBD-BODIPY}} = 2720 \text{ M}^{-1} \text{ s}^{-1}$. With this key value in-hand, the data in Figure 1 can be analyzed using the well-established kinetic expressions for inhibited hydrocarbon autoxidations,^{3–5} where k_{inh} for the RTAs can be determined from the initial rate of PBD-BODIPY consumption as in eq 12 and n from t_{inh} as in eq 13:⁵¹

$$\frac{-\delta[\text{PBD-BODIPY}]}{\delta t} = \frac{k_{\text{PBD-BODIPY}}[\text{PBD-BODIPY}]R_i}{nk_{\text{inh}}[\text{RTA}]} \quad (12)$$

$$n = \frac{t_{\text{inh}}R_i}{[\text{RTA}]} \quad (13)$$

Doing so for RTAs 2–4 yields rate constants that are within experimental error of those determined by O_2 consumption (see Table 1) and which are characterized by stoichiometric numbers of $n \sim 2$, as expected (*vide supra*). RTA 1 (BHT) was too slow to effectively compete with PBD-BODIPY oxidation, precluding determination of its corresponding k_{inh} value (more on this later).

To demonstrate the utility of the approach for carrying out mechanistic studies, we determined example kinetic isotope effects (KIE) and kinetic solvent effects for the well-known reaction of 3. The KIE for the reaction of 3 with peroxy radicals was obtained by the addition of 1% MeOH/MeOD to an

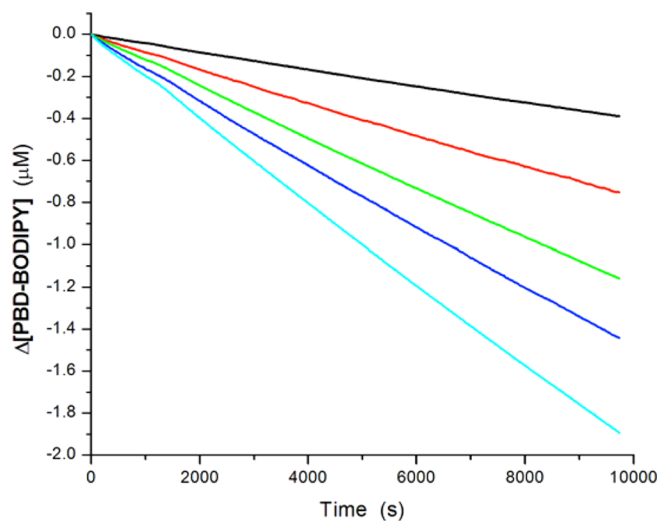
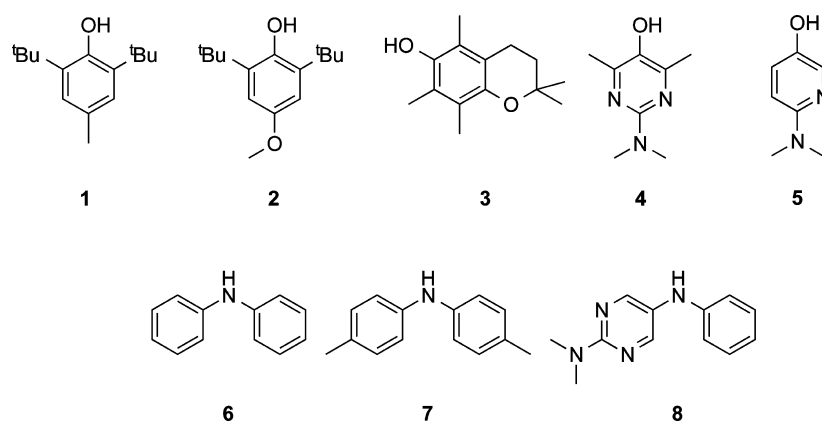


Figure 2. Rate of PBD-BODIPY consumption as a function of PBD-BODIPY concentration in AIBN-initiated (6 mM) co-oxidations of PBD-BODIPY and styrene (4.3 M) in PhCl at 37 $^{\circ}\text{C}$ (left) and the corresponding representative raw data (right). Reaction progress was monitored by absorbance at 591 nm ($\epsilon = 139,000 \text{ M}^{-1} \text{ cm}^{-1}$).

Table 1. Inhibition Rate Constants and Stoichiometries Determined for Various RTAs Determined by Co-oxidations of PBD-BODIPY and Styrene^a

RTA	<i>n</i>	k_{inh} ($\text{M}^{-1} \text{s}^{-1}$)	lit. k_{inh} ($\text{M}^{-1} \text{s}^{-1}$)
1	too slow	too slow	1.4×10^4 (30 °C) ²⁴
2	1.8 ± 0.2	$(1.6 \pm 0.2) \times 10^5$	1.1×10^5 (30 °C) ²⁴
3	2.0	$(3.8 \pm 0.2) \times 10^6$	3.8×10^6 (30 °C) ²⁴
3 ^b	1.9 ± 0.1	$(8.1 \pm 0.8) \times 10^5$	7.5×10^5 (30 °C) ^d
3 ^c	2.0	$(6.6 \pm 0.4) \times 10^5$	6.8×10^5 (30 °C) ²⁵
4	1.8 ± 0.1	$(9.9 \pm 2.3) \times 10^6$	7.4×10^6 (30 °C) ²⁶
5	2.0 ± 0.2	$(4.4 \pm 0.6) \times 10^6$	3.6×10^6 (30 °C) ²⁶
6	too slow	too slow	2.0×10^4 (65 °C) ²⁷
7	3.1 ± 0.2	$(3.7 \pm 0.2) \times 10^5$	1.8×10^5 (37 °C) ²⁸
8	3.9 ± 0.2	$(9.9 \pm 0.6) \times 10^5$	3.0×10^6 (37 °C) ²⁸

^aDetermined by co-oxidation of styrene (4.3 M) and PBD-BODIPY (10 μM) initiated by AIBN (6 mM) in PhCl at 37 °C and inhibited by 1–2 μM RTA. ^bSame as above, but containing 1% MeOD. The corresponding value for 1% MeOH was $k_{\text{inh}} = (3.6 \pm 0.2) \times 10^6 \text{ M}^{-1} \text{ s}^{-1}$. The literature value was determined for 1% D₂O/H₂O. ^cMeasured in CH₃CN. ^dCalculated from literature data.^{24,29}

inhibited autoxidation. While MeOH had only a slight effect on the inhibition rate constant, $k_{\text{inh}}(\text{PhCl})/k_{\text{inh}}(\text{PhCl} + \text{MeOH}) = 1.1$, addition of MeOD substantially lowered it, i.e. $k_{\text{inh}}(\text{PhCl} + \text{MeOH})/k_{\text{inh}}(\text{PhCl} + \text{MeOD}) = k_{\text{H}}/k_{\text{D}} = 4.4$, in good agreement with the literature value of 5.1²⁹ and consistent with significant O–H bond cleavage in the transition state of the reaction of phenols with peroxy radicals (eq 3). When the autoxidation was carried out in acetonitrile in lieu of chlorobenzene, $k_{\text{inh}}(\text{CH}_3\text{CN}) = 6.6 \times 10^5 \text{ M}^{-1} \text{ s}^{-1}$ was obtained—a kinetic solvent effect of $k_{\text{PhCl}}/k_{\text{MeCN}} = 5.8$, in good agreement with the literature value of 5.6,^{24,25} and consistent with the existence of a hydrogen-bonded pre-equilibrium.¹²

In order to further validate the current approach to assessing RTA activity, we also sought to reproduce an example of synergy between RTAs since this is often not picked up in simple antioxidant assays.³⁰ We chose an example from a recent investigation on antioxidant synergism carried out with our collaborators:²⁶ the combination of a highly reactive pyridinol RTA (5) with a much less reactive hindered phenol (2). The data are shown in Figure 3, and are fully consistent with results obtained by O₂ consumption measurements.²⁶ That is, although the pyridinol is a fine RTA on its own, the hindered phenol can only retard oxidation of PBD-BODIPY. However, when the two RTAs are used together, their performance is much better than their additive contributions. This arises because the less reactive hindered phenol regenerates the more reactive pyridinol *in situ*, as in eq 14. This equilibrium is favorable since the O–H bond in pyridinol 5 is stronger than the O–H bond in hindered phenol 2 (by 2.4 kcal/mol).²⁶

Diarylamine RTAs were also considered in our method validation. Representative inhibited autoxidation traces are

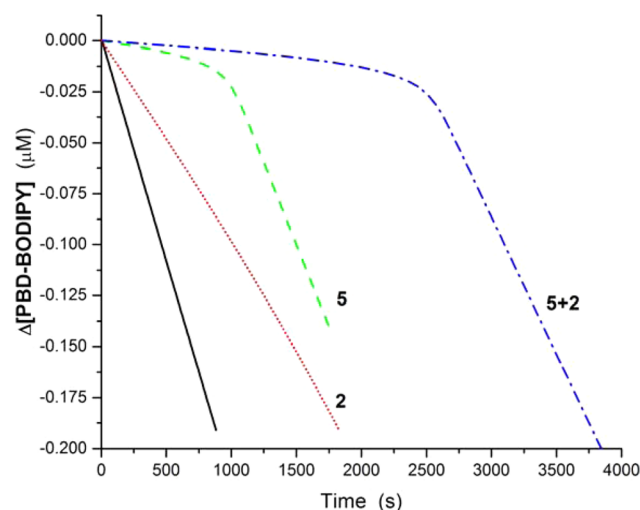


Figure 3. Co-oxidation of styrene (4.3 M) and PBD-BODIPY (10 μM) initiated by AIBN (6 mM) in PhCl at 37 °C (solid line) and inhibited by 2 (2 μM), 5 (1 μM), or 5 + 2 (1 μM + 2 μM). Reaction progress was monitored by absorbance at 591 nm ($\epsilon = 139,000 \text{ M}^{-1} \text{ cm}^{-1}$).

shown in Figure 4. Like BHT, diphenylamine was too slow to effectively inhibit PBD-BODIPY oxidation. 4,4'-Dimethyldiphenylamine (7), representative of the industrial standard dialkylated diphenylamines, displayed a pronounced inhibited period, as did the recently described heteroaryl-containing diarylamine 8.²⁸ The rate constants obtained from fitting the data were in good agreement with the literature values (see Table 1).³¹ Interestingly, the stoichiometric numbers from these experiments ($n = 3.1$ for 7 and $n = 3.9$ for 8) suggest that

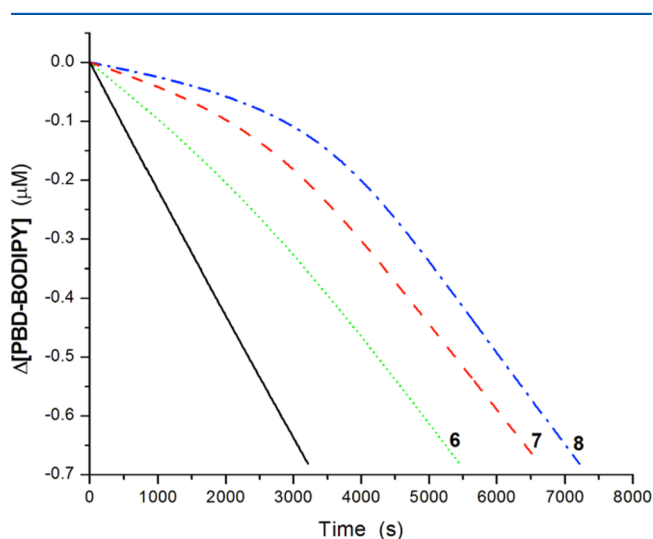
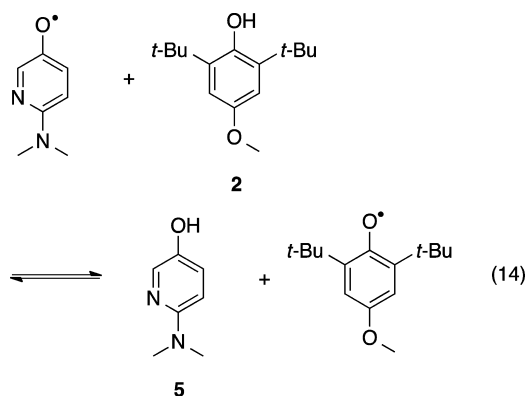
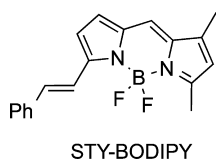


Figure 4. Co-oxidation of styrene (4.3 M) and PBD-BODIPY (10 μM) initiated by AIBN (6 mM) in PhCl at 37 $^{\circ}\text{C}$ (solid line) and inhibited by 2 μM of 6, 7 and 8. Reaction progress was monitored by absorbance at 591 nm ($\epsilon = 139,000 \text{ M}^{-1} \text{ cm}^{-1}$).

more than two peroxy radicals are trapped by each molecule of RTA, consistent with previous inhibited autoxidations monitored by O_2 consumption.²⁸ The basis of this behavior remains unclear, but is likely to be related to the catalytic behavior exhibited by diarylamines at elevated temperatures.^{32,33}

Monitoring Slower Autoxidations. Since PBD-BODIPY reacts too quickly with chain-carrying peroxy radicals to be able to report on the potency of moderately reactive (and widely used) RTAs such as BHT and diphenylamine, we sought to develop a slightly less reactive analogue. We surmised that the removal of one of the unsaturations in the 1-phenylbutadiene sidechain in PBD-BODIPY should decrease its reactivity to peroxy radical addition significantly. We therefore prepared the styryl analogue, STY-BODIPY, for use as the signal carrier in an analogous co-oxidation procedure employing cumene ($k_p = 0.34 \text{ M}^{-1} \text{ s}^{-1}$)¹⁶

Cumylperoxy radicals undergo significantly slower termination reactions than styrylperoxy radicals (i.e., $k_t = 2.3 \times 10^4 \text{ M}^{-1} \text{ s}^{-1}$ vs. $2.1 \times 10^7 \text{ M}^{-1} \text{ s}^{-1}$),³⁴ resulting in a higher steady



state concentration of radicals and a concomitant increase in the rate at which STY-BODIPY is consumed. However, slower termination of chain-carrying radicals implies that cross-termination between cumylperoxy radicals and secondary peroxy radicals derived from STY-BODIPY will contribute significantly to the steady-state concentration of radicals in the autoxidation. Therefore, the direct determination of $k_{\text{STY-BODIPY}}$ could not be carried out as we did to obtain $k_{\text{PBD-BODIPY}}$. Instead, $k_{\text{STY-BODIPY}}$ was determined from the inhibited co-oxidation of STY-BODIPY and cumene (Figure 5).

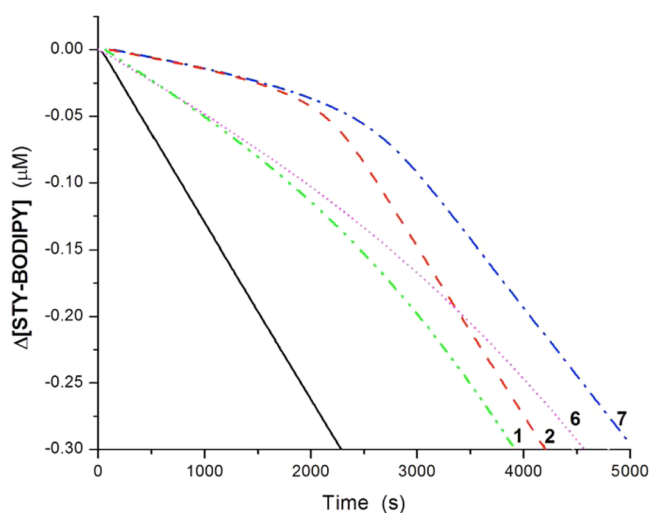


Figure 5. Co-oxidation of cumene (3.6 M) and STY-BODIPY (10 μM) initiated by AIBN (6 mM) in PhCl at 37 $^{\circ}\text{C}$ (solid line) and inhibited by 2 μM of BHT (1), (2) and diarylamines 6 and 7. Reaction progress was monitored by absorbance at 571 nm ($\epsilon = 128,000 \text{ M}^{-1} \text{ cm}^{-1}$).

Since 2 is known to have $k_{\text{inh}} = 1.1 \times 10^5 \text{ M}^{-1} \text{ s}^{-1}$ and a stoichiometric number of $n = 2$,²⁴ the rate constant could be obtained simply by fitting the data to the standard kinetic scheme for inhibited autoxidations modified to include the contribution of chain propagation from the reaction of STY-BODIPY with peroxy radicals (see the [Supporting Information](#) for complete details). Fitting of this data yields $k_{\text{STY-BODIPY}} = 141 \text{ M}^{-1} \text{ s}^{-1}$. This rate constant indicates that STY-BODIPY is significantly less reactive than PBD-BODIPY (recall $k_{\text{PBD-BODIPY}} = 2720 \text{ M}^{-1} \text{ s}^{-1}$)—as expected—but still more reactive than styrene itself ($41 \text{ M}^{-1} \text{ s}^{-1}$) and much more reactive than cumene ($k_p = 0.34$),²³ its co-oxidation substrate.

Co-oxidations of STY-BODIPY and cumene were well-behaved and yielded inhibition rate constants for test RTAs that were in very good agreement with values obtained from O_2 consumption.³⁵ As expected, the slower rate of probe oxidation enabled the determination of rate constants for the slower RTAs BHT (1) and diphenylamine (6), which did not yield discernible inhibited periods in the autoxidation of the more reactive probe, PBD-BODIPY (cf. Figures 1 and 4, respectively).³⁶ Some representative data are shown in Table 2.

Autoxidations in Water. Although PBD-BODIPY and STY-BODIPY are highly lipophilic, the very small concentrations used in the styrene and cumene co-oxidations prompted us to consider if they would be useful for monitoring the kinetics of inhibited autoxidations in aqueous media. Kinetic data for the reactions of peroxy radicals in water are relatively sparse despite their purported importance *in vivo*. Most data are

Table 2. Inhibition Rate Constants and Stoichiometries Determined for Various RTAs Determined by Co-oxidations of STY-BODIPY and Cumene^a

RTA	<i>n</i>	<i>k</i> _{inh} (M ⁻¹ s ⁻¹)	lit. <i>k</i> _{inh} (M ⁻¹ s ⁻¹)
1	2.2 ± 0.1	(2.1 ± 0.2) × 10 ⁴	1.4 × 10 ⁴ (30 °C) ²⁴
2	2.1 ± 0.1	1.1 × 10 ^{5b}	1.1 × 10 ⁵ (30 °C) ²⁴
6	2.5 ± 0.1	(1.7 ± 0.2) × 10 ⁴	2.0 × 10 ⁴ (65 °C) ²⁷
7	2.4 ± 0.1	(1.1 ± 0.1) × 10 ⁵	1.8 × 10 ⁵ (37 °C) ²⁸

^aDetermined by inhibited co-oxidation of cumene (3.6 M) and STY-BODIPY (10 μM) initiated by AIBN (6 mM) in PhCl at 37 °C and inhibited by 2 μM antioxidant. ^bAssumed in order to derive *k*_{STY-BODIPY}.

derived from pulse radiolysis measurements where kinetics for the reactions of RTAs with methylperoxyl, and more often the highly reactive trichloromethylperoxyl, radicals have been determined.³⁷

Co-oxidations of STY-BODIPY and THF as a 40% (by volume) solution in water³⁸ initiated by the water-soluble azo initiator AAPH were very well behaved and consumption of STY-BODIPY was expectedly inhibited by the water-soluble antioxidants, Trolox (9) and ascorbate (10), see Figure 6.

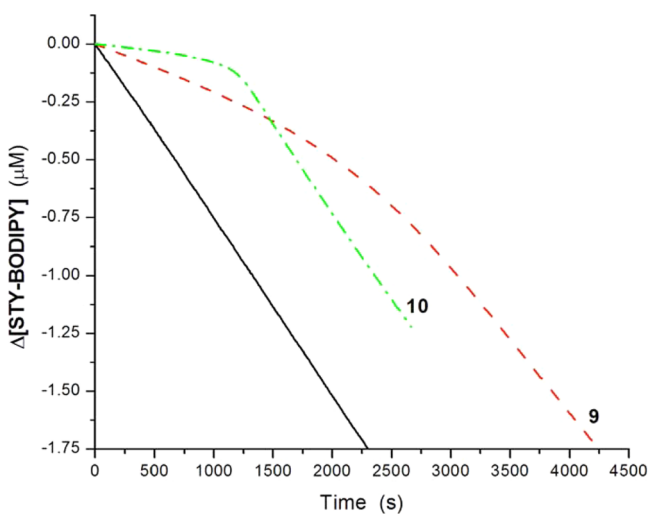
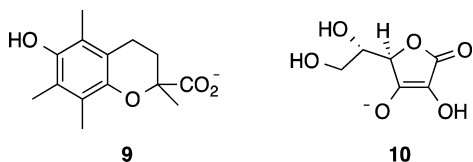


Figure 6. Co-oxidation of THF (4.9 M) and STY-BODIPY (10 μM) initiated with AAPH (1 mM) in water at 37 °C (solid line) and inhibited by 2 μM of 9 or 20 μM of 10. Reaction progress was monitored by absorbance at 562 nm ($\epsilon = 147,000 \text{ M}^{-1} \text{ cm}^{-1}$).

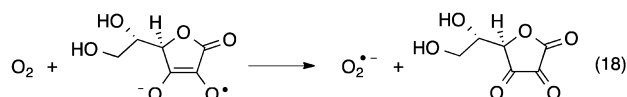
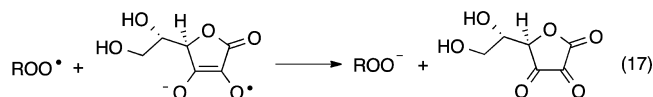
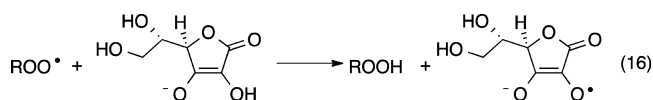


As was the case in the foregoing experiments, determination of inhibition rate constants in this system requires knowledge of the rate constant for reaction of STY-BODIPY with THF-derived peroxy radicals (*k*_{STY-BODIPY}). Accordingly, data from ascorbate-inhibited autoxidations were fit to the standard kinetic scheme for inhibited autoxidations of THF (*k*_p = 4.4 M⁻¹ s⁻¹)^{39–41} modified to include the contribution of chain-propagation from reaction of STY-BODIPY with the THF-derived peroxy radicals. Using the literature rate constant for the reaction of ascorbate and methylperoxyl radical obtained by pulse radiolysis

measurements ($2.4 \times 10^6 \text{ M}^{-1} \text{ s}^{-1}$),⁴² a value of *k*_{STY-BODIPY} = $7.9 \times 10^3 \text{ M}^{-1} \text{ s}^{-1}$ was calculated.⁴³ Using this value, the inhibition rate constant for Trolox was measured to be *k*_{inh} = $2.2 \times 10^5 \text{ M}^{-1} \text{ s}^{-1}$, in very good agreement with the value predicted for α -tocopherol ($4.9 \times 10^5 \text{ M}^{-1} \text{ s}^{-1}$) using the relationship developed by Ingold and co-workers for kinetic solvent effects on H atom transfer reactions (eq 15) and the constants *k*_{inh}⁰ = $7.2 \times 10^6 \text{ M}^{-1} \text{ s}^{-1}$, α_2^{H} (α -TOH) = 0.37 and β_2^{H} (H₂O) = 0.38.^{12,44}

$$\log k_{\text{inh}}^{\text{S}} = \log k_{\text{inh}}^0 - 8.3\alpha_2^{\text{H}}\beta_2^{\text{H}} \quad (15)$$

Under the reaction conditions, the stoichiometry of the ascorbate/peroxy reaction was found to be only ~0.1. Although ascorbate can, in principle, reduce two peroxy radicals to form dehydroascorbic acid (as in eqs 16 and 17), low stoichiometric



numbers are commonly observed for ascorbate—either alone ($n \rightarrow 0$ as [ascorbate] $\rightarrow \infty$)⁴⁵ or when used in a synergistic combination with a lipid-soluble compound such as α -TOH.⁴⁶ The lower than ideal stoichiometry has been ascribed to the autoxidation of ascorbate and/or the reaction of the ascorbyl radical (anion) with O₂ to yield a chain carrying hydroperoxyl radical (superoxide, eq 18) in competition with the reaction of the ascorbyl radical (anion) with another peroxy radical.^{45,46} The methods described herein may prove useful in delineating this reaction mechanism as well as others that have yet to be studied in detail in aqueous media.

CONCLUSION

We have developed a novel, accurate, and operationally simple method for the study of antioxidant reactivity by the inhibited autoxidation approach. Reaction progress is monitored continuously by following the consumption of an easily synthesized BODIPY-conjugated probe by visible light spectrophotometry. The inhibition rate constants measured for several phenol and diarylamine RTAs using this approach are in excellent agreement with literature values. The method describes the co-antioxidant behavior of RTA mixtures and also the enhanced stoichiometry of suitably reactive diarylamines. The method can be calibrated for use in solvents of different polarities and/or H-bonding properties, allowing measurements of kinetic solvent effects. Furthermore, deuterium kinetic isotope effects are easily measured by the addition of 1% MeOD/MeOH to the co-oxidations. Overall, the approach enables any researcher with access to a conventional UV–vis spectrophotometer to carry out inhibited hydrocarbon autoxidations to obtain invaluable kinetic and stoichiometric data on RTAs. It is our hope that this method will supplant popular assays based on spectroscopic determinations of equilibria between RTAs and persistent radicals or similarly dubious assessments of “antioxidant activity”.

EXPERIMENTAL SECTION

General Methods. All chemicals and solvents were purchased from commercial suppliers and used without further purification. Styrene and cumene were purified in batches. Styrene was extracted three times with 1 M NaOH_(aq) and washed with water before drying with MgSO₄ and filtering. It was then fractionally distilled under vacuum, percolated through a column of silica, and stored under nitrogen at -20 °C (it could be stored for up to 3–4 days prior to use). It was further percolated through a column of ~1/3 silica gel layered on top of ~2/3 basic alumina immediately prior to use. Cumene was purified by the same method. Commercially available phenolic antioxidants BHT, BHA, and PMC (1, 2, and 3) were recrystallized prior to use. 6-(Dimethylamino)-3-pyridinol (4), 2-(dimethylamino)-4,6-dimethyl-5-pyrimidinol (5), and N²,N²-dimethyl-N⁵-phenylpyrimidine-2,5-diamine (8) were synthesized by the reported procedures.^{47,48} Diphenylamine (6) and di-*p*-tolylamine (7) were purchased and used without further purification. UV-vis spectra and kinetics were measured on a UV-vis spectrophotometer equipped with a temperature controller unit and a thermostated 6 × 6 multicell holder.

Synthesis of PBD- and STY-BODIPY. Both compounds were synthesized by literature procedures.^{16,17} Briefly, a solid mixture of pyrrole-2-carboxaldehyde⁴⁹ (1.0 g, 10.5 mmol), zinc dust (0.69 g, 10.5 mmol), and either cinnamyl triphenylphosphonium chloride or benzyl triphenylphosphonium bromide (4.3 or 4.5 g, 10.5 mmol) was heated to 100 °C under an inert atmosphere and stirred overnight. The mixture was allowed to cool before it was diluted with CHCl₃ (25 mL) and filtered. The filtrate was washed once with water and once with brine before drying with MgSO₄. Following filtration and concentration under reduced pressure, the product was purified by column chromatography on silica gel using a gradient of 20–30% CHCl₃ in hexanes.

The product phenylbutadienyl- or styryl-substituted pyrrole (0.53 or 0.46 g, 2.7 mmol) was then combined with 3,5-dimethylpyrrole-2-carboxaldehyde (0.34 g, 2.7 mmol) in dry CH₂Cl₂ (135 mL) under an inert atmosphere. POCl₃ (0.27 mL, 2.9 mmol) was then added dropwise over several minutes, and the reaction was stirred overnight in the dark at room temperature. Diisopropylethylamine (2.0 mL, 11.5 mmol) was then added slowly, and the reaction was stirred for another 10 min, followed by dropwise addition of BF₃-OEt₂ (1.4 mL, 11.2 mmol). The reaction was stirred at room temperature until complete (~1 h, as judged by TLC), poured into a separatory funnel, and washed twice with water and then a small amount of brine. The organic phase was dried with MgSO₄ and filtered and the solvent evaporated. Column chromatography (100% CH₂Cl₂) removed the major impurities. A second column (60% CH₂Cl₂ in hexanes) afforded pure product.

Due to the oxidizability of both PBD-BODIPY and STY-BODIPY, 2.0 mM stock solutions of each compound were prepared in either 1,2,4-trichlorobenzene or DMSO (depending on whether they are for use in organic or aqueous solutions) and stored under nitrogen, frozen at -20 °C. When stored in this manner, there was minimal background oxidation of the either compound over several months.

4,4-Difluoro-5,7-dimethyl-3-(4-phenyl-1,3-butadienyl)-4-bora-3a,4a-diaza-s-indacene (PBD-BODIPY). Yield: 81 mg (9%). ¹H NMR (400 MHz; acetone-*d*₆): δ 7.65 (d, *J* = 7.3 Hz, 2H), 7.51 (s, 1H), 7.43–7.32 (m, 5H), 7.21–7.15 (m, 2H), 7.06 (d, *J* = 4.7 Hz, 1H), 6.94 (d, *J* = 14.9 Hz, 1H), 6.30 (s, 1H), 2.58 (s, 3H), 2.33 (s, 3H). ¹⁹F NMR (377 MHz; acetone-*d*₆, PhCF₃ standard): δ -143.16 (dd, *J* = 65.6, 32.8 Hz). HRMS (EI - magnetic sector): calcd for C₂₁H₁₅BF₂N₂ 348.16094, found 348.15828. λ_{max} (PhCl) = 591 nm, ε = 139162 M⁻¹ cm⁻¹. The poor solubility of PBD-BODIPY in either CDCl₃, DMSO, acetone, or benzene, combined with its high oxidizability, prevented the acquisition of a well-resolved ¹³C NMR spectrum.

4,4-Difluoro-5,7-dimethyl-3-(2-phenylethenyl)-4-bora-3a,4a-diaza-s-indacene (STY-BODIPY). Yield: 128 mg (15%). ¹H NMR (400 MHz; acetone-*d*₆): δ 7.64 (t, *J* = 10.9 Hz, 3H), 7.52 (t, *J* = 8.2 Hz, 2H), 7.44 (t, *J* = 7.5 Hz, 2H), 7.36 (t, *J* = 7.3 Hz, 1H), 7.15 (d, *J* = 4.3 Hz, 1H), 7.08 (d, *J* = 4.4 Hz, 1H), 6.29 (s, 1H), 2.57 (s, 3H), 2.31 (s, 3H). ¹³C NMR (75 MHz; acetone-*d*₆): δ 159.2, 153.0, 143.6, 136.7, 135.3, 135.0, 128.93, 128.85, 128.71, 127.0, 123.2, 120.2, 119.0, 115.2, 14.0, 10.4. ¹⁹F NMR (377 MHz; acetone-*d*₆): δ -143.00 (dd, *J* = 69.6 Hz, 34.8 Hz).

HRMS (EI - magnetic sector): calcd for C₁₉H₁₇BF₂N₂ 322.14529, found 322.14342. λ_{max} (PhCl) = 571 nm, ε = 128,141 M⁻¹ cm⁻¹.

Inhibited Co-oxidations: Styrene/Cumene. Freshly purified styrene or cumene (1.25 mL) was loaded into a 3 mL cuvette along with 1.18 mL of PhCl. The cuvette was placed into the thermostated sample holder of a UV-vis spectrophotometer and allowed to equilibrate to 37 °C. A small aliquot (12.5 μL) of a 2.0 mM solution of the BODIPY probe in 1,2,4-trichlorobenzene was added, followed by 50 μL of 0.3 M solution of AIBN in PhCl, and the solution was thoroughly mixed. The absorbance at either 591 nm (PBD-BODIPY) or 571 nm (STY-BODIPY) was monitored for 40–60 min to ensure that the reaction was proceeding at a constant rate, after which 10 μL of a 500 μM solution of the test antioxidant was added. The solution was thoroughly mixed and the absorbance readings resumed.

Inhibited Co-oxidations: THF/H₂O. Unstabilized THF (1.0 mL) was loaded into a 3 mL cuvette along with 1.43 mL of H₂O. The cuvette was placed into the thermostated sample holder of a UV-vis spectrophotometer and allowed to equilibrate to 37 °C. A small aliquot (12.5 μL) of a 2.0 mM solution of the BODIPY probe in DMSO was added, followed by 50 μL of 0.05 M solution of AAPH in H₂O, and the solution was thoroughly mixed. The absorbance at 562 nm was monitored for 10–20 min to ensure that the reaction was proceeding at a constant rate, after which 10 μL of a 500 μM solution of the test antioxidant was added. The solution was thoroughly mixed, and the absorbance readings were resumed.

ASSOCIATED CONTENT

Supporting Information

The Supporting Information is available free of charge on the ACS Publications website at DOI: 10.1021/acs.joc.5b02183.

UV-vis and NMR spectra of PBD-BODIPY and STY-BODIPY, details of kinetic modeling and parameter fitting (COPASI), and optimized geometries and energies for computational results (PDF)

AUTHOR INFORMATION

Corresponding Author

*E-mail: dpratt@uottawa.ca.

Notes

The authors declare no competing financial interest.

ACKNOWLEDGMENTS

We thank the Natural Sciences and Engineering Research Council of Canada (NSERC), the Canada Foundation for Innovation, and the Canada Research Chairs program for financial support. E.A.H. thanks the Government of Ontario for award of an Ontario Graduate Scholarship, and A.V.K. thanks NSERC for an Undergraduate Student Research Award.

REFERENCES

- Ingold, K. U. *Chem. Rev.* **1961**, *61*, 563–589.
- Ingold, K. U.; Pratt, D. A. *Chem. Rev.* **2014**, *114*, 9022–9046.
- Valgimigli, L.; Pratt, D. A. In *Encyclopedia of Radicals in Chemistry, Biology and Materials*; Chatgililoglu, C., Studer, A., Eds.; John Wiley & Sons.: Chichester, UK, 2012.
- Li, B.; Pratt, D. A. *Free Radical Biol. Med.* **2015**, *82*, 187–202.
- Amorati, R.; Valgimigli, L. *Free Radical Res.* **2015**, *49*, 633–649.
- Hanthorn, J. J.; Haidasz, E.; Gebhardt, P.; Pratt, D. A. *Chem. Commun.* **2012**, *48*, 10141–10143.
- Re, R.; Pellegrini, N.; Proteggente, A.; Pannala, A.; Yang, M.; Rice-Evans, C. *Free Radical Biol. Med.* **1999**, *26*, 1231–1237.
- Benzie, I. F.; Strain, J. J. *Anal. Biochem.* **1996**, *239*, 70–76.
- Blois, M. S. *Nature* **1958**, *181*, 1199–1200.
- Huang, D.; Ou, B.; Prior, R. L. *J. Agric. Food Chem.* **2005**, *53*, 1841–1856.
- Foti, M. J. *J. Agric. Food Chem.* **2015**, *63*, 8765–8776.

- (12) Litwinienko, G.; Ingold, K. U. *Acc. Chem. Res.* **2007**, *40*, 222–230.
- (13) Kang, H. C.; Haugland, R. P. Long Wavelength Chemically Reactive Dipyrrometheneboron Difluoride Dyes and Conjugates. US5451663 A, 1993.
- (14) Drummen, G. P.; van Liebergen, L. C.; Op den Kamp, J. A.; Post, J. A. *Free Radical Biol. Med.* **2002**, *33*, 473–490.
- (15) Yoshida, Y.; Shimakawa, S.; Itoh, N.; Niki, E. *Free Radic. Res.* **2003**, *37*, 861–872.
- (16) Kang, H. C.; Haugland, R. P. Ethenyl-Substituted Dipyrrometheneboron Difluoride Dyes and Their Synthesis. US5187288, 1993.
- (17) De Cremer, G.; Roefsaers, M. B. J.; Bartholomeeusen, E.; Lin, K.; Dedeker, P.; Pescarmona, P. P.; Jacobs, P. A.; De Vos, D. E.; Hofkens, J.; Sels, B. F. *Angew. Chem., Int. Ed.* **2010**, *49*, 908–911.
- (18) Naguib, Y. M. *Anal. Biochem.* **1998**, *265*, 290–298.
- (19) DFT calculations using the B3LYP/CBSB7 method indicate that the most favorable position for peroxy addition is adjacent to the phenyl ring, yielding an allyl-BODIPY radical at least 7.4 kcal/mol more stable than those radicals derived from addition of the peroxy radical at any of the other three positions of the 1-phenylbutadiene moiety. See the [Supporting Information](#) for further details.
- (20) Moreover, in some preliminary inhibited co-oxidations the fluorescence intensity was significantly suppressed even when no/minimal inhibition was expected to take place. This was likely the result of fluorescence quenching by some RTAs and/or their oxidation products.
- (21) Hammond, G. S.; Sen, J. N.; Boozer, C. E. *J. Am. Chem. Soc.* **1955**, *77*, 3244–3248.
- (22) Van Hook, J. P.; Tobolsky, A. V. *J. Am. Chem. Soc.* **1958**, *80*, 779–782.
- (23) Howard, J.; Ingold, K. *Can. J. Chem.* **1967**, *45*, 793–802.
- (24) Burton, G. W.; Doba, T.; Gabe, E.; Hughes, L.; Lee, F. L.; Prasad, L.; Ingold, K. U. *J. Am. Chem. Soc.* **1985**, *107*, 7053–7065.
- (25) Valgimigli, L.; Amorati, R.; Petrucci, S.; Pedulli, G. F.; Hu, D.; Hanthorn, J. J.; Pratt, D. A. *Angew. Chem., Int. Ed.* **2009**, *48*, 8348–8351.
- (26) Valgimigli, L.; Bartolomei, D.; Amorati, R.; Haidasz, E.; Hanthorn, J. J.; Nara, S. J.; Brinkhorst, J.; Pratt, D. A. *Beilstein J. Org. Chem.* **2013**, *9*, 2781–2792.
- (27) Brownlie, I. T.; Ingold, K. U. *Can. J. Chem.* **1966**, *44*, 861–868.
- (28) Hanthorn, J. J.; Amorati, R.; Valgimigli, L.; Pratt, D. A. *J. Org. Chem.* **2012**, *77*, 6895–6907.
- (29) Burton, G. W.; Ingold, K. U. *J. Am. Chem. Soc.* **1981**, *103*, 6472–6477.
- (30) Equilibrium methods (such as those used in many of the most common “antioxidant activity” assays) only reflect the reaction stoichiometry and show only additive relationships between multiple antioxidants.
- (31) The literature value for 8^{28} was determined using a peroxy radical clock approach,⁵⁰ which was found to overestimate the rate constants for some of the more reactive diarylamines relative to data obtained from inhibited autoxidations (by a factor of 2–3).²⁸
- (32) Jensen, R. K.; Korcek, S.; Zinbo, M.; Gerlock, J. L. *J. Org. Chem.* **1995**, *60*, 5396–5400.
- (33) Haidasz, E. A.; Shah, R.; Pratt, D. A. *J. Am. Chem. Soc.* **2014**, *136*, 16643–16650.
- (34) Enes, R. F.; Tomé, A. C.; Cavaleiro, J. A. S.; Amorati, R.; Fumo, M. G.; Pedulli, G. F.; Valgimigli, L. *Chem. - Eur. J.* **2006**, *12*, 4646–4653.
- (35) Diarylamine **7** showed reduced stoichiometry in these experiments relative to the PBD-BODIPY/styrene co-oxidations ($n = 2.4$ vs 3.1). Secondary alkyl radicals (or the alkoxyamines derived from their combination with diarylnitroxides) are necessary for either the retro-carbonyl-ene or homolysis/dis-proportionation reaction to complete the catalytic cycle.^{27,28} Similarly, the more reactive diarylamine **8** completely inhibited the reaction and had a stoichiometric number, $n = 2.3$, also down considerably from 3.9 in the PBD-BODIPY/styrene co-oxidations.
- (36) The more reactive RTAs **3–5** and **8** completely inhibited the co-oxidation reaction, precluding determination of the inhibition rate constants.
- (37) von Sonntag, C.; Schuchmann, H.-P. *Angew. Chem., Int. Ed. Engl.* **1991**, *30*, 1229–1253. Neta, P.; Huie, R. E.; Ross, A. B. *J. Phys. Chem. Ref. Data* **1990**, *19*, 413–513.
- (38) The selection of this system was inspired by the work of Valgimigli and Amorati communicated at the 2014 International Congress on Hydrogen Atom Transfer (Rome).
- (39) Howard, J. A.; Ingold, K. U. *Can. J. Chem.* **1969**, *47*, 3809–3815.
- (40) Howard, J. A. *Adv. Free Radical Chem.* **1972**, *4*, 49–173.
- (41) The propagation rate constant in THF/H₂O was assumed to be the same as in neat THF. R_i was determined from t_{inh} in the autoxidation inhibited by Trolox and assuming $n = 2$. See ref 24.
- (42) Alfassi, Z. B.; Huie, R. E.; Kumar, M.; Neta, P. *J. Phys. Chem.* **1992**, *96*, 767–770.
- (43) The rate constant for the reaction of STY-BODIPY with THF-derived peroxy radicals is significantly higher than that of STY-BODIPY with cumylperoxy radicals also in chlorobenzene, where it was measured to be $2.0 \times 10^3 \text{ M}^{-1}\text{s}^{-1}$ (versus $141 \text{ M}^{-1}\text{s}^{-1}$ for cumylperoxyls). The difference (13.8-fold) can be rationalized by the greater electrophilicity of the THF-derived peroxy radical compared to the cumylperoxyl radical and the significant polar effects known to operate in the transition states of radical additions to alkenes. For a discussion, see: Russell, G. A. In *Free Radicals*; Kochi, J. K., Ed.; Wiley: New York, 1973; Vol. 1, pp 275–332.
- (44) Snelgrove, D. W.; Luszytky, J.; Banks, J. T.; Mulder, P.; Ingold, K. U. *J. Am. Chem. Soc.* **2001**, *123*, 469–477.
- (45) See: Wayner, D. D. M.; Burton, G. W.; Ingold, K. U. *Biochim. Biophys. Acta, Gen. Subj.* **1986**, *884*, 119–123 and references cited therein.
- (46) Doba, T.; Burton, G. W.; Ingold, K. U. *Biochim. Biophys. Acta, Lipids Lipid Metab.* **1985**, *835*, 298–303. Barclay, L. R. C.; Locke, S. J.; MacNeil, J. M. *Can. J. Chem.* **1983**, *61*, 1288–1290.
- (47) Nam, T.-G.; Nara, S. J.; Zagol-Ikapitte, I.; Cooper, T.; Valgimigli, L.; Oates, J. A.; Porter, N. A.; Boutaud, O.; Pratt, D. A. *Org. Biomol. Chem.* **2009**, *7*, 5103–5112.
- (48) Hanthorn, J. J.; Valgimigli, L.; Pratt, D. A. *J. Org. Chem.* **2012**, *77*, 6908–6916.
- (49) Ryskiewicz, R. M.; Silverstein, E. E.; Willard, C. *Org. Synth.* **1956**, *36*, 74.
- (50) Hanthorn, J. J.; Pratt, D. A. *J. Org. Chem.* **2012**, *77*, 276–284.
- (51) Alternatively, the data in [Figure 1](#) can be fit numerically to the standard kinetic scheme for inhibited autoxidations^{3–5} modified to include the contribution of chain propagation from the reaction of PBD-BODIPY with peroxy radicals in order to derive k_{inh} for the RTAs (see the [Supporting Information](#) for complete details). The two approaches yield indistinguishable data.